Journal of The Electrochemical Society, **156** (4) A253-A259 (2009)
0013-4651/2009/156(4)/A253/7/$23.00 © The Electrochemical Society

Electrochemical Comparison and Deposition of Lithium and Potassium from Phosphonium- and Ammonium-TFSI Ionic Liquids

Jose A. Vega, Junfeng Zhou, and Paul A. Kohl[*,z]

School of Chemical and Biomolecular Engineering, Georgia Institute of Technology, Atlanta, Georgia 30332-0100, USA

Two room-temperature ionic liquids, $Bu_3HexP^+TFSI^-$ [TFSI = bis(trifluoromethanesulfonyl)imide] and $Bu_3HexN^+TFSI^-$, were synthesized and their electrochemical behavior was investigated using CV. The phosphonium-based ionic liquid (IL) showed improved stability and physical properties compared to the analogous ammonium-based IL. The phosphonium-based IL had higher conductivity (0.43 mS/cm) than the ammonium-based IL (0.28 mS/cm). The lower viscosity and higher stability of the phosphonium-based IL led to higher current density and stability for electrodeposited lithium metal. The addition of LiTFSI to both ILs led to a decrease in conductivity and increase in viscosity. An optimum deposition potential was found that was bounded by the electrochemical stability of each IL. The stability of lithium in the ILs increased at lower temperature due to slower reactivity with the IL. The electrodeposition and reoxidation of potassium was also demonstrated. It was found that a lithium-potassium alloy could be deposited at high current for long times without the occurrence of dendrites.
 [DOI: 10.1149/1.3070657]

Manuscript submitted November 4, 2008; revised manuscript received December 17, 2008. Published January 30, 2009.

The need for high power and energy density batteries for electronics applications has increased attention for lithium metal-based batteries. These batteries are desirable because lithium has a low molecular weight, provides a more negative anode potential, and has a higher theoretical capacity than its Li-intercalated carbon counterpart. However, there are significant technological issues that need to be addressed. Safety is a concern due to the volatility and flammability of the conventional nonaqueous organic electrolytes that are typically used in these batteries. Electrodes using lithium metal are prone to forming dendrites when recharged.[1-3] This can lead to electrode shorting, high short-circuit current, heat generation, and thermal runaway.

Ionic liquids (ILs) can be used as electrolytes for electrochemical devices because they are nonflammable and have high thermal and chemical stability with no vapor pressure.[4,5] ILs can be used for the electroplating of metals that would otherwise react with water, such as sodium or lithium. Also, the wide electrochemical stability of ILs allows for a combination of lithium metal anodes with the conventional intercalation cathodes. The chemical and physical properties can be altered by changing the cation or anion structure.

A wide variety of imidazolium and quaternary (Quat) ammonium ILs have been studied for sodium[6,7] and lithium[5,8] electrodeposition. $Quats^+$ are especially attractive because of the wide range of structures that can be obtained through alkylation of the tertiary amines.[9,10]

Two of the most studied IL anions for lithium and sodium deposition are chloroaluminate ($AlCl_4^-$) and bistrifluoromethanesulfonimide ($TFSI^-$). Chloroaluminate-based ILs are formed via a Lewis acid-base reaction between an organic halide $Quat^+$ and $AlCl_3$. This family of ILs also requires the presence of an additive, such as thionyl chloride or hydrochloric acid, to enable metal plating. An excess of $AlCl_3$ is added in order to create an acidic IL containing $Al_2Cl_7^-$ that can be neutralized by addition of NaCl or LiCl; this provides the source of metal ions for electrodeposition to the metallic state. $TFSI^-$-based ILs are formed via ion exchange between the organic halide $Quat^+$ and lithium bistrifluoromethanesulfonimide (LiTFSI). Metals other than lithium may also be used. They do not require the presence of an additive for metal plating to occur. Simple dissolution of the metal-TFSI salt in the IL provides the source of metal ions for electrodeposition.

Although ammonium ILs have been widely studied, few reports can be found concerning phosphonium ILs.[11,12] Phosphonium ILs are interesting because they provide higher conductivity and electrochemical stability than their ammonium counterparts.[13] As a consequence, these ILs may provide improved performance in the electrochemical deposition and reoxidation of metals. Also, the feasibility of lithium electrodeposition and reoxidation from phosphonium ILs has recently been demonstrated.[14] Therefore, it is of interest to investigate the electrochemical aspects of phosphonium ILs and their response to different experimental conditions to determine their potential as electrolytes.

The suppression of dendrites is essential for lithium secondary batteries with a metallic anode.[15] Electrodeposition of other metals, such as zinc, tin, and silver, also allows the formation of dendrites.[16-18] Metallic dendrites have been related to short circuits that cause electronic system failures. Dendrite suppression in other metals has been achieved by creating alloys consisting of the primary metal and a small amount of a secondary metal. For example, tin-lead is a reliable system for soldering;[19] and zinc-nickel is used for corrosion resistance.[20] Previously, lithium dendrite suppression has been achieved in chloroaluminate ILs by forming a lithium-sodium alloy.[21] Also, lithium dendrite suppression was recently reported by use of a lithium-magnesium alloy, where no dendrites were observed after continuous cycling of the electrode.[22]

In this study, the electrochemical behavior of two room-temperature ILs, $Bu_3HexP^+TFSI^-$ and $Bu_3HexN^+TFSI^-$, was investigated. These two ILs were chosen so that a direct comparison can be made between a quaternary phosphonium and ammonium for the deposition of lithium and a lithium alloy. The counter anion used in this investigation was $TFSI^-$, which was chosen due to its high electrochemical stability. Both ILs were studied via cyclic voltammetry (CV). The stability of lithium metal in the ILs was studied to investigate the relative stability of the two ILs and to show the viability of forming a lithium metal anode for use in a battery. Also, a lithium-potassium alloy was investigated as a means of preventing dendrite formation.

Experimental

Synthesis of the phosphonium IL was carried out by reaction of tri-n-butylphosphine with 1-bromohexane with no solvent present. The reaction mechanism is summarized in Fig. 1. The reaction was carried out at 70°C for seven days in a round-bottom flask, and a quaternary phosphonium bromide was obtained. The remaining reactants were removed by washing three times with diethyl ether. By-products were removed by mixing the IL with activated carbon followed by filtration. This step was repeated several times until the final product was colorless. The bromide anion was exchanged for $TFSI^-$ in an aqueous solution by mixing the quaternary phospho-

* Electrochemical Society Fellow.
z E-mail: kohl@gatech.edu

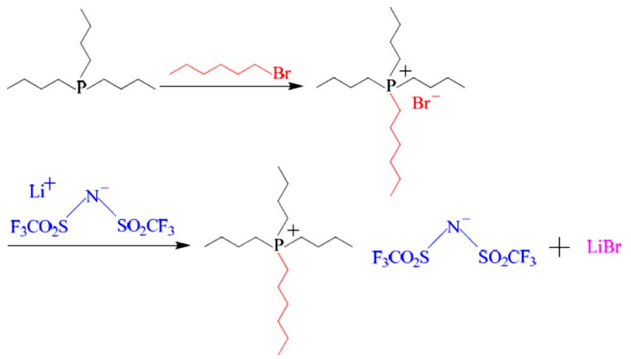

Figure 1. (Color online) Synthesis route for $Bu_3HexP^+TFSI^-$ IL.

nium bromide with LiTFSI for one day to yield a phosphonium Quat with a $TFSI^-$ anion. Lithium bromide was removed in the aqueous phase. The phosphonium IL was hydrophobic and was washed with high-purity water. The IL and water phase were separated, and silver nitrate was added to the aqueous phase to test for residual bromide. The presence of silver bromide precipitate in the aqueous phase indicated that bromide remained in the IL phase. The IL was repeatedly washed until no silver bromide precipitate was observed. The IL was dried under vacuum at 70°C for 48 h. Finally, the sample was stored in a dry nitrogen-atmosphere glove box. The preparation and purification of other ILs was carried out in the same way except that the appropriate staring phosphine or amine was chosen.

The ILs were characterized by Fourier transform IR and NMR spectroscopy. Density measurements were obtained by using a precalibrated picnometer (2.03 mL at 25°C). Viscosity measurements were performed using a slow-flow viscometer (Cannon Instruments). Melting points were determined by continuously monitoring the temperature with a thermocouple while the liquid was cooled and observing when a liquid-solid phase change occurred. The experiments above and below room temperature were performed with a custom-built cell and an ISOTEMP 3016 for temperature control.

LiTFSI was obtained from Acros Organics and potassium bis(trifluoromethanesulfonyl)imide (KTFSI) was obtained from Wako Chemicals. Both salts were recrystallized and dried under vacuum before being placed in the glove box. Dissolution of LiTFSI in the IL required stirring for 3 h at room temperature. Dissolution of KTFSI required overnight stirring at 100°C.

Conductivity measurements were performed with a ThermoOrion conductivity meter and a custom-built probe with platinum plates set at a fixed distance apart and with the corners sealed in glass. Calibration was performed with a KCl calibration solution before use in the glove box. After each use, the probe was cleaned with hot nitric acid, rinsed with deionized (DI) water, and dried in an oven.

An EG&G model 263A potentiostat was used to perform the electrochemical measurements inside the glove box. A tungsten working electrode was fabricated by sealing a tungsten wire (0.5 mm diam) in a glass tube. Prior to use, the electrode was cleaned with hot nitric acid, polished with 0.3 μm alumina powder, and thoroughly rinsed with DI water. The counter electrode was a platinum foil sealed with glass around the corners, and the reference electrode was a silver wire. The CV experiments were typically performed at a scan rate of 10 mV/s. Cobalticinium (Cc) hexafluorophosphate (10 mM) was used as an internal reference electrode. All potentials were reported vs the Cc/Cc^+ couple. The silver wire pseudoreference electrode was placed close to the working electrode. The resistivity of the IL was a strong function of temperature and concentration of dissolved salts, as shown in the Results section. Thus, it was difficult to perform internal resistance (iR) corrections, especially for the deposition or reoxidation of lithium because the IL resistivity changed during the experiment. Thus, the current-voltage curves were presented without iR correction. The small electrode area mitigated the overall uncompensated resistance effect.

For the electrochemical experiments involving lithium, a flame test was performed to prove its presence in the electrode. The electrode containing lithium was immersed in DI water to dissolve the metal. A platinum wire was immersed in the metal-containing solution and placed into a blue flame.

Results

The melting point and viscosity of quaternary ammonium ILs are affected by the size and nature of the alkyl substituents, and the overall symmetry of the ions.[23] This is because the ability of the IL to crystallize depends on the nature and shape of the substituents. In this study, it is of interest to compare the physical and electrochemical stability of quaternary ammonium and phosphonium ILs. A specific quaternary ammonium and analogous phosphonium IL were selected for detailed study. However, first a series of quaternary phosphonium–TFSI ILs were prepared and their melting points were determined. $Bu_3ProP^+TFSI^-$, $Bu_4P^+TFSI^-$, $Bu_3PenP^+TFSI^-$, and $Bu_3HexP^+TFSI^-$ were synthesized from tri-n-butylphosphine. The melting points for the four ILs were 65, 80, 34, and −18°C, respectively. Thus, the $Bu_3HexP^+TFSI^-$ IL was chosen because of its low melting point. The analogous ammonium IL was synthesized so that a direct comparison could be made between an ammonium and phosphonium IL with the same substituents and anion. The melting point of $Bu_3HexN^+TFSI^-$ was found to be −6°C. The physical properties of the two ILs are given in Table I. The phosphonium-based IL was treated once with activated carbon to remove impurities, and the ammonium-based IL was purified with activated carbon four times. The final ILs were transparent with a yellow tint, which was removed by the carbon treatment. The difference in viscosity between the two ILs is striking. The higher viscosity for the ammonium-based IL will certainly affect the diffusivity and mobility of ions within the IL, as can be seen in the higher conductivity of the phosphonium-based IL.

The electrochemical stability of $Bu_3HexP^+TFSI^-$ and $Bu_3HexN^+TFSI^-$ IL was evaluated in two ways. First, CV was used to examine the stability of the neat IL. Second, LiTFSI was added to each IL and lithium was electrochemically deposited. The stability of the electrodeposited lithium in the IL was used as a probe of the stability of the IL to electroreduction. The stability of lithium metal is also of interest when considering these ILs as electrolytes in a lithium metal battery.

Figure 2 shows the voltammetric response for both ILs using a 0.5 mm diam tungsten working electrode. The electrochemical stability, as indicated by the onset potential for reduction of the ILs, is virtually the same at 25°C, with the onset at about −1.9 V vs Cc/Cc^+. The background current at potentials positive of −1.9 V in

Table I. Physical properties of the ILs.

IL	Molecular weight	Melting point (°C)	Density at 25°C ρ (g/mL)	Molar concentration *C* (mol/L)	Viscosity at 25°C η (cP)	Ionic conductivity at 25°C σ (mS/cm)
$Bu_3HexP^+TFSI^-$	567.70	−18	1.18	2.08	261	0.43
$Bu_3HexN^+TFSI^-$	550.74	−6	1.19	2.16	397	0.28

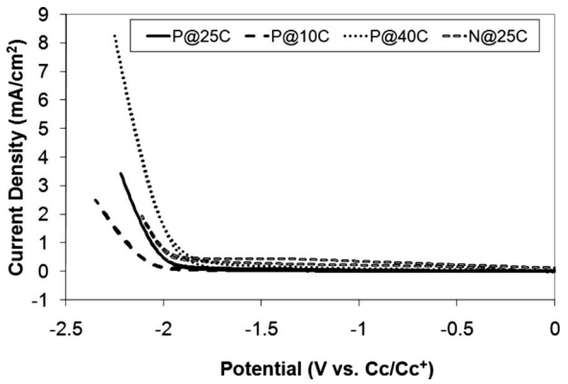

Figure 2. CV for neat $Bu_3HexP^+TFSI^-$ and $Bu_3HexN^+TFSI^-$.

the ammonium-based IL was slightly higher than for the phosphonium-based IL. At higher temperatures, the onset potential for IL reduction shifts to more positive values. At lower temperatures, the reduction of the IL is slower, as reflected in the shift in current to more negative potentials. The reduction of both ILs is an irreversible reaction, on the time scale of the CVs performed here. That is, no reoxidation current was observed on the positive-going reverse scans. Thus, there is little difference in the electrochemical behavior of the two ILs, when measured for stability at a tungsten electrode.

The electrodeposition of lithium from the ILs and stability of lithium metal in the presence of the ILs was investigated. Lithium ions were added to the IL by dissolving LiTFSI in the IL. The conductivity of each IL was measured as a function of the LiTFSI concentration at 25°C. The LiTFSI concentration was from 0.0 to 1.0 M for the ammonium-based IL and 0.0 to 1.5 M for the phosphonium IL. LiTFSI was not as soluble in the ammonium-based IL. Figure 3 shows the change in conductivity with LiTFSI concentration. The measurements were each performed two times, and the average value is reported. The difference between the values measured for each IL was 4% different for phosphonium-based IL and 3% different for the ammonium-based IL. The rate of decrease in conductivity with LiTFSI is essentially the same for the two ILs. The decrease in conductivity was accompanied by an increase in viscosity. The viscosity of the neat phosphonium-based IL was 261 cP and nearly tripled, 747 cP, with 1.5 M LiTFSI. This follows the comparable increase in resistivity (essentially triple) by addition of LiTFSI. The neat ammonium IL had a viscosity of 397 and 1583 cP with 1 M LiTFSI. This trend follows previous results with

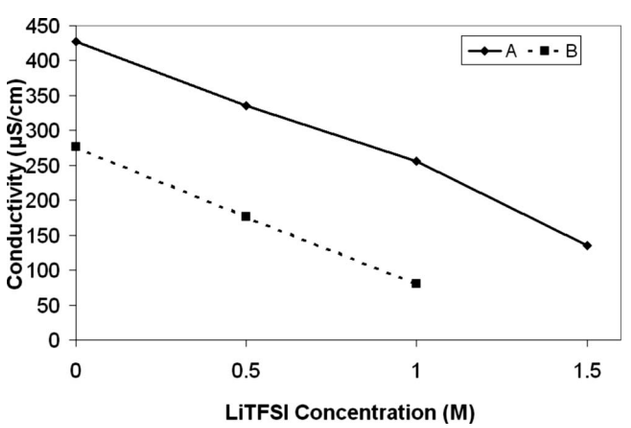

Figure 3. Ionic conductivity at 25°C vs different Li^+ concentrations for (A) $Bu_3HexP^+TFSI^-$ and (B) $Bu_3HexN^+TFSI^-$.

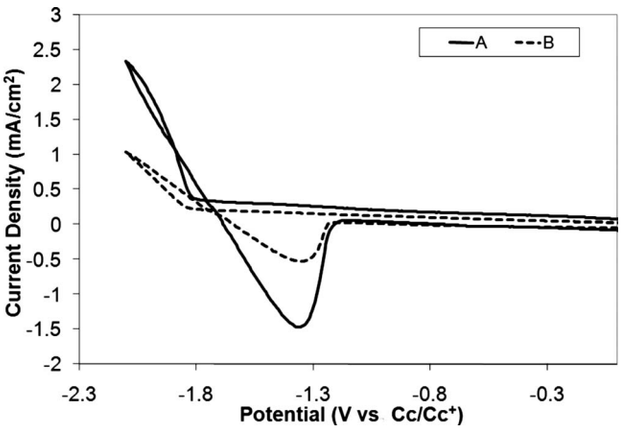

Figure 4. CV for (A) $Bu_3HexP^+TFSI^-$ and (B) $Bu_3HexN^+TFSI^-$ containing 1 M LiTFSI at 25°C and switching potential of −2.1 V.

other ILs, where the addition of small cations increased the resistivity.[9] This trend is different from solvent-solute systems, where smaller ions have higher conductivity.

The electrochemical behavior of a tungsten electrode in the LiTFSI IL is quite different from the neat IL. Figure 4 shows the CV response in the phosphonium- and ammonium-based ILs with 1M LiTFSI at 25°C. The switching potential for the CV was −2.1 V. The magnitude of the reduction current at potentials negative of −1.8 V is greater than the background scans shown in Fig. 2 at the same temperature. No correction for uncompensated resistance was performed, as noted in the Experimental section. The higher resistance of the ammonium-based IL contributes to the more gradual rise in current compared to the phosphonium-based IL. The resistance of IL was further complicated by the dependence of the resistivity on LiTFSI concentration, as shown in Fig. 3. That is, as lithium is removed from the IL by deposition, the resistivity of the IL decreases, making iR compensation not possible for a full scan. A hysteresis in the reduction current and an anodic peak were observed following the reduction process. These observations are consistent with the reduction and reoxidation of lithium metal.[21] The hysteresis in the reduction curves has been attributed to an overpotential for the reduction when lithium is first deposited on a foreign surface (i.e., tungsten). The anodic peak is due to reoxidation of the lithium metal deposited during the reduction process. The reduction of lithium ions to lithium metal is superimposed on the small background reduction current, which is due to impurities, as observed with the neat ILs in Fig. 2. The onset of lithium-ion reduction in Fig. 4 occurs at a slightly more positive potential (e.g., −1.8 V) compared to Fig. 2. Flame tests were performed, as described earlier, to verify the presence of lithium on the working electrode. Immersion of the metal electrode in DI water caused the formation of gas bubbles, consistent with the reaction of lithium with water forming hydrogen gas. A platinum wire was immersed in the metal-containing solution and placed into a blue flame. Lithium produces a red flame, which was clearly observed when the wire was exposed to the flame.

Coulombic efficiencies are a practical method of investigating the stability of the lithium deposition and reoxidation process. Here, the coulombic efficiency is defined as the ratio of oxidation charge due to lithium stripping divided by the lithium reduction charge. The coulombic efficiencies were calculated from the CV curves using two methods. First, the efficiencies were calculated using only cathodic and anodic currents. That is, the reduction charge includes the reduction of the impurities in the IL. The oxidation charge was obtained from the integral of the negative current, such as in Fig. 4. The inclusion of the background impurity current will give an overly pessimistic value of lithium stability. This is referred to as method 1.

Table II. Coulombic efficiencies for both ILs at 25°C with 1 M LiTFSI concentration using both calculation methods.

	Efficiency (%)			
	Method 1		Method 2	
Switching potential (V)	$Bu_3HexP^+TFSI^-$	$Bu_3HexN^+TFSI^-$	$Bu_3HexP^+TFSI^-$	$Bu_3HexN^+TFSI^-$
−1.9	11	—	77	—
−2	30	16	67	62
−2.1	45	32	63	56
−2.2	46	39	59	50

Because the impurity current may not be present during battery operation, a second method was used to calculate the efficiencies that more closely resembles the true stability of lithium. The coulombic efficiency was calculated from the area under the cathodic and anodic current curves using the impurity background current as a baseline. That is, the near linear current-potential curve at potentials positive of −1.8 V was extrapolated to −2.1 V. This presumably would be the coulombic efficiency if the impurity were not present in the IL. This is referred to as method 2.

Table II shows the coulombic efficiencies at different switching potentials for 1 M LiTFSI in the ILs at 25°C using both calculation methods. The measurements were performed two times, and the highest value is reported. The results were very reproducible with the difference between the two values being <2% of the total. The coulombic efficiency of lithium reduction and reoxidation was slightly higher for the phosphonium IL than the ammonium IL. Method 2 probably provides a more accurate comparison of the two ILs because it compensates for a different level of background impurity. The loss of coulombic efficiency could be due to direct reduction of the IL or reaction between the lithium and the IL. In either case, the more stable IL should yield higher coulombic efficiency. Figure 2 shows that the IL is reduced at tungsten in this potential range. Other losses of coulombic efficiency include lithium dendrites falling off the electrode. These secondary loss mechanisms were hard to validate or quantify.

When the switching potential is made more negative (Table II), the efficiency increases using method 1 simply because the overall current becomes large compared to the background current. However, using method 2, the coulombic efficiency decreases slightly at more negative potentials because the reduction of the IL (see Fig. 2) begins to become more appreciable. Recall that at potentials where the IL can be reduced, it has a substantial concentration advantage compared to the concentration of Li^+. Although the true potential is slightly different from that shown in Table II due to a small uncompensated resistance, the trend and conclusions are very clear.

On the basis of the higher coulombic efficiency for lithium (Table II) and lower direct reduction current of the phosphonium-based IL (Fig. 2), it is reasonable to conclude that the phosphonium IL is electrochemically more stable at negative potentials than the analogous ammonium IL. Because the only difference between the two mixtures is the nitrogen vs phosphorous portion of the ion, one is drawn to the slightly larger size of the phosphonium center and resulting lower charge density (i.e., lower nucleophilic attack). The lower charge density may also be the origin of the lower viscosity and higher solubility of LiTSFI because there is somewhat less of a tendency for ion pairing.

The electrochemical response as a function of temperature is of interest because it may give insight into the relative competition between lithium-ion reduction and IL reduction, and it is of interest for potential battery applications. Figure 5 shows the CV response for 0.5 M LiTFSI dissolved in the phosphonium- and ammonium-based ILs at different temperatures. The switching potential in each experiment was −2.1 V. The magnitude of the reduction and oxidation currents depends on temperature mainly because the viscosity and mobility of the ions is different. The change in temperature also had an effect on the coulombic efficiency of lithium. Table III shows the coulombic efficiencies for the phosphonium- and ammonium-based ILs with 0.5 M LiTFSI at different temperatures and switching potentials using method 2 as the basis for calculation. In each case, the phosphonium-based IL was more stable than the corresponding ammonium-based IL. The highest efficiencies measured in the phosphonium-based IL were 84 and 35% for the ammonium-based IL, which occurred at 10°C. At high temperature, 40°C, the stability of lithium in the ILs decreased and a lower fraction of lithium metal was recovered. Although this may be solely due to that fact that lithium-ion reduction is more competitive with direct IL reduction at lower temperature (i.e., the rate of IL reduction decreases more with temperature than the rate of lithium-ion reduction), the lower current density may also be a contributory factor because of secondary effects at high current (e.g., material falling off the electrode).

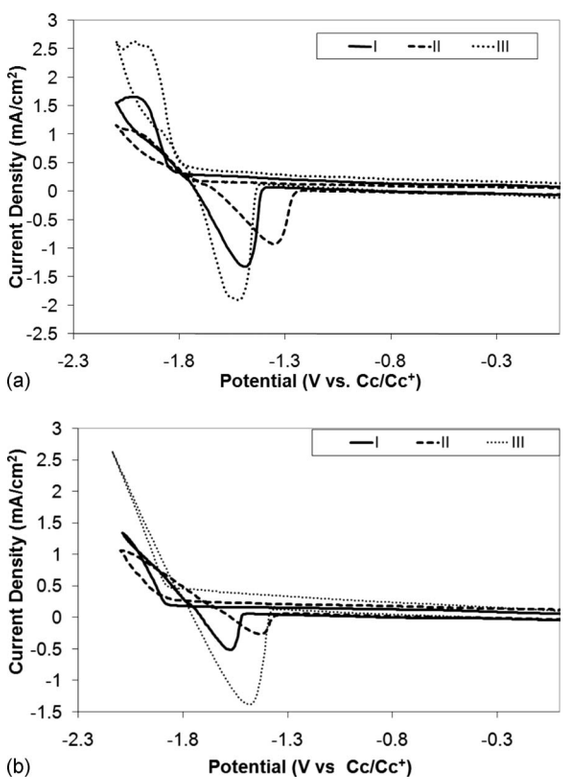

Figure 5. CV at (I) 25, (II) 10, and (III) 40°C, 0.5 M LiTFSI concentration, and switching potential = −2.1 V for (A) $Bu_3HexP^+TFSI^-$ and (B) $Bu_3HexN^+TFSI^-$.

Table III. Coulombic efficiencies at different temperatures for both ILs with 0.5 M LiTFSI.

	Efficiency (%)					
	$Bu_3HexP^+TFSI^-$			$Bu_3HexN^+TFSI^-$		
Switching potential (V)	10°C	25°C	40°C	10°C	25°C	40°C
−1.9	84	74	67	—	—	—
−2	77	62	63	35	30	28
−2.1	66	60	48	29	23	24
−2.2	—	—	—	21	17	17

It is interesting to note that a mass-transfer limited current peak is observed only in the phosphonium-based IL, as shown in Fig. 5. This shows that Li^+ reduction is favored over IL reduction, which is consistent with the higher coulombic efficiency for lithium-ion reduction shown in Table III. That is, the mass-transport–limited condition can be reached for the phosphonium-based IL because a greater faction of the current goes to Li^+ reduction (vs IL reduction) before the onset of significant IL reduction.

The diffusion-limited, Li^+ peak was confirmed by increasing the concentration of LiTFSI to 1.0 and 1.5 M at 25°C, as shown in Fig. 6. The switching potential for each scan was −2.1 V. The cathodic and resulting reoxidation current increased when the Li^+ concentration was increased from 0.5 to 1.0 M because there is a greater amount of Li^+ available for reduction. However, the current decreased on further addition of LiTFSI due to the increase in viscosity and resulting decrease in diffusivity of Li^+, as shown by the conductivity decrease in Fig. 3. The same trend was observed in the ammonium-based IL, as shown in Fig. 7. An increase in the LiTFSI concentration from 0.5 to 1 M caused a decrease in the cathodic current and resulting anodic peak current.

If the cathodic current at potentials negative of −1.9 V were a competition between the reduction of the IL and Li^+, then one would expect to see a difference in coulombic efficiency with LiTFSI concentration. Table IV gives the coulombic efficiency in each IL as a function of the Li concentration and switching potential using method 2 as the basis for calculation. When the LiTFSI concentration was increased, the fraction of reduction current resulting in lithium metal available for reoxidation increased. The ammonium-based IL had a larger increase in efficiency with LiTFSI concentration because the IL reduction is more competitive (greater fraction going to IL reduction than Li^+ reduction) than for the phosphonium-based IL reduction.

Previous studies have reported the reduction of sodium ions and codeposition of a lithium-sodium alloy.[6,7] In this work, potassium-only and lithium-potassium alloy electrodeposition were investigated. The deposition of potassium has been previously reported on a mercury electrode by Scordillis-Kelley et al.; they did not observe deposition on tungsten.[24] Potassium electrodeposition and reoxidation were observed on a tungsten electrode using the phosphonium-based IL containing 0.25 M KTFSI at 25°C with a switching potential of −2.3 V, as shown in Fig. 8. The onset for potassium-ion–only deposition (ca. −2.1 V) occurs at a more negative potential than the lithium-ion reduction (ca. −1.8 V). The presence of an anodic peak following the scan to negative potentials shows that potassium metal was deposited during the reduction process.

The codeposition of Li–K was investigated using a phosphonium-based IL with 0.075 M KTFSI and 1.5 M LiTFSI. The CV at a tungsten electrode with and without the addition of the 0.075 M KTFSI is shown in Fig. 9 at 25°C and switching potential of −2.3 V. The onset potential for alloy deposition was slightly more positive than for lithium or potassium alone. The standard potential for the deposition of an alloy can be different from that of the individual metals because of a lower Gibbs free energy for the alloy process. The shift in deposition potential to more positive values also resulted in an increase in the coulombic efficiency because the metal deposition competes more effectively with IL reduction at the more positive potentials, as shown in Table V.

The increase in coulombic efficiency for the Li–K alloy may also have a contribution from an improved morphology of the deposited metal. That is, lithium is known to form dendrites whereas the alloying metal can suppress dendrite formation. The working electrode was visually examined for dendrite growth. Particular care was taken during these observations because dendrites can be fragile. The electrode was maintained inside the IL during observation and the cell was not moved so as to minimize vibrations. The experiment

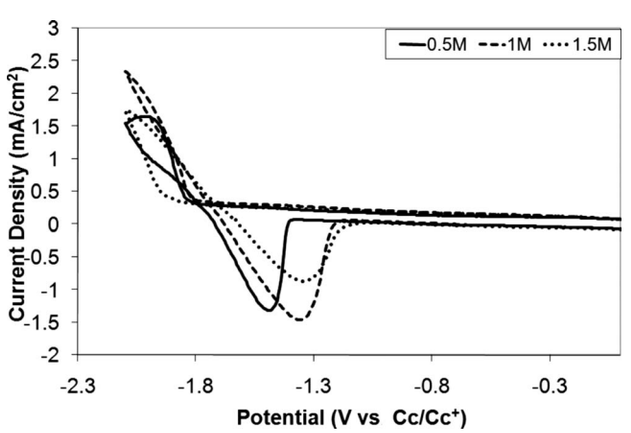

Figure 6. CV for $Bu_3HexP^+TFSI^-$ IL at different LiTFSI concentrations, temperature of 25°C, and switching potential = −2.1 V.

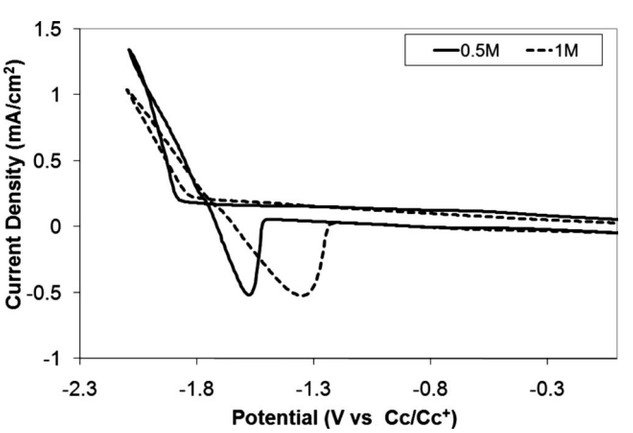

Figure 7. CV for $Bu_3HexN^+TFSI^-$ IL at different LiTFSI concentrations, temperature of 25°C, and switching potential = −2.1 V.

Table IV. Coulombic efficiencies for different LiTFSI concentrations in both IL at 25°C

	Efficiency (%)				
	Bu_3HexP^+ $TFSI^-$			Bu_3HexN^+ $TFSI^-$	
Switching potential (%)	0.5 M	1 M	1.5 M	0.5 M	1 M
−1.9	74	77	80	—	69
−2	62	67	69	30	62
−2.1	60	63	67	23	56
−2.2	—	—	61	17	50

consisted of constant reduction at 1.5 mA/cm^2 for 30 min. Dendrites were clearly observed on the electrode surface when the IL contained 1.5 M LiTFSI only (no KTFSI present). The deposit was rough and had a needlelike morphology. When the electrode was gently shaken, a portion of the deposited metal could be seen falling off the surface of the electrode.

When KTFSI was added to the IL (1.5 M LiTFSI and 0.075 M KTFSI) and the experiment was repeated (1.5 mA/cm^2 for 30 min), no dendrites were observed under the same conditions using the same observation techniques. The surface of the electrode had a smooth and uniform deposit. When the experiment was extended to 60 min deposition time, no dendritic growth was observed.

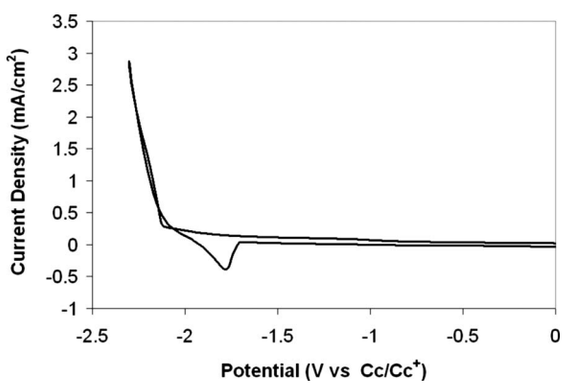

Figure 8. CV for $Bu_3HexP^+TFSI^-$ IL at 25°C, 0.25 M KTFSI and switching potential of −2.3 V.

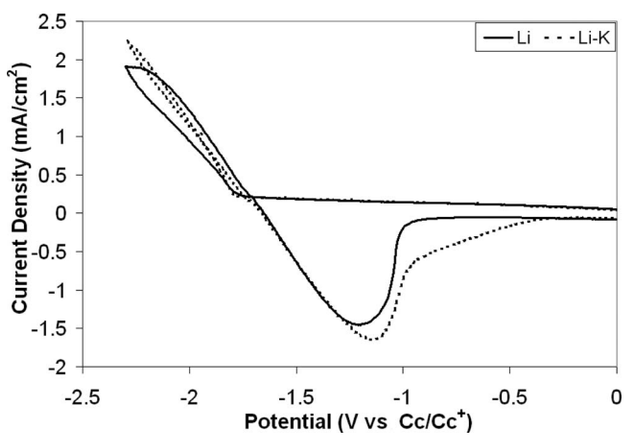

Figure 9. CV for $Bu_3HexP^+TFSI^-$ IL with 1.5 M LiTFSI and 0.075 M KTFSI at 25°C and switching potential of −2.2 V.

Discussion

A direct comparison of the physical and electrochemical properties between a quaternary ammonium- and phosphonium-based IL showed several interesting differences. During synthesis and purification, the phosphonium-based IL was easier to synthesize and required fewer steps and shorter times to purify. The direct electrochemical reduction of the neat ILs showed only a small difference, which is reasonable based on the subtle difference in structure of the two ILs. In both cases, the wide temperature window is highly beneficial for electrochemical devices.

The physical property differences are especially striking. The phosphonium-based IL has a significantly higher conductivity and lower viscosity compared to the ammonium-based IL over the entire range of Li^+ concentrations (Fig. 3). Tsunashima and Sugiya argued that this higher conductivity is due to lower electrostatic interaction between the phosphonium cation and the $TFSI^-$ anion, in comparison to the ammonium cation.[13] The subtitle difference is N^+ vs P^+ size (and resulting difference in charge density) has a dramatic effect on the ion-ion interactions. Less anion-cation attraction would result in higher mobility of the ions in the IL and lower overall viscosity (Table I).[25]

The sensitivity to anion-cation interaction is also shown when lithium cations are added to the ILs. In a dilute, solvent-solute electrolyte, smaller ions generally have higher mobility so that replacing large ions with smaller ones results in higher conductivity. Here, the addition of a relatively small number of lithium ions (e.g., 0.5 M) leads to dramatic reduction in conductivity and increase in viscosity. This same effect of lower conductivity by replacing large ions with smaller ones has been observed in other ILs.[7] The ILs are very sensitive to electrostatic interactions of the ions because there is no solvent present to help distribute the charge over larger volumes. This is a particular concern in electrochemical devices based on small ions (e.g., Li^+) because they have the smallest mass (leading to high energy density devices) and have the highest mobility in the solvent-solute electrolytes.

The decrease in mobility of small ions (and increase in viscosity of the IL) with lithium-ion addition also creates coulombic efficiency problems. The concentration of IL at the electrode surface during reduction remains essentially fixed and does not rely on dif-

Table V. Coulombic efficiency for phosphonim IL at 25°C before and after addition of potassium.

	Efficiency (%)	
Switching potential (V)	1.5 M LiTFSI	1.5 M LiTFSI & 0.075 M KTFSI
−2	69	80
−2.1	67	78
−2.2	61	70
−2.3	58	63

fusion to the same extent as Li^+ transport relies on diffusion. Thus, higher viscosity and lower mobility will lead to lower coulombic efficiencies, a situation unfavorable to battery applications.

Alloy formation has several benefits for battery applications. First, the shift of the reduction potential to more positive values is an advantage because the metal reduction is better able to compete with electrolyte reduction, resulting in higher cycling efficiency and lower self-discharge. Previous work has demonstrated that ILs lacking sufficient cathodic stability were not able to undergo electrodeposition and reoxidation of metals[26] or showed very poor performance.[27] The second advantage of alloy formation is the suppression of dendrites. The feasibility of potassium metal deposition on a tungsten electrode has been shown here (Fig. 8). Dendrite suppression is an essential attribute for a lithium-metal anode in a battery.

Conclusion

The use of a phosphonium-based IL had several advantages over the analogous ammonium-based IL. The phosphonium IL had higher conductivity and lower viscosity than the ammonium-based IL, which led to higher current densities. The addition of LiTFSI to the IL caused a decrease in the conductivity and increase in viscosity. The coulombic efficiency for lithium electrodeposition and reoxidation was higher in the phosphonium IL. The feasibility of potassium deposition and reoxidation was shown. The addition of a small amount of potassium ions to an IL with lithium ions shifted the reduction potential for the alloy to more positive values, giving an increase in the coulombic efficiency compared to lithium alone. Deposition of a lithium-potassium alloy occurred without the formation of dendrites under the conditions where lithium alone formed dendrites.

Georgia Institute of Technology assisted in meeting the publication costs of this article.

References

1. M. Dollé, L. Sannier, B. Beaudoin, M. Trentin, and J. Tarascon, *Electrochem. Solid-State Lett.*, **5**, A286 (2002).
2. C. Brissot, M. Rosso, J. Chazalviel, P. Baudry, and S. Lascaud, *Electrochim. Acta*, **43**, 1569 (1998).
3. C. Brissot, M. Rosso, J. Chazalviel, and S. Lascaud, *J. Power Sources*, **81–82**, 925 (1999).
4. H. Sakaebe, H. Matsumoto, and K. Tatsumi, *Electrochim. Acta*, **53**, 1048 (2007).
5. S. Seki, Y. Kobayashi, H. Miyashiro, Y. Ohno, A. Usami, Y. Mita, N. Kihira, M. Watanabe, and N. Terada, *J. Phys. Chem. B*, **110**, 10228 (2006).
6. G. Gray, J. Winnick, and P. Kohl, *J. Electrochem. Soc.*, **143**, 2262 (1996).
7. K. Kim, C. Lang, and P. Kohl, *J. Electrochem. Soc.*, **152**, E9 (2005).
8. S. Seki, Y. Kobayashi, H. Miyashiro, Y. Ohno, Y. Mita, A. Usami, N. Terada, and M. Watanabe, *Electrochem. Solid-State Lett.*, **8**, A577 (2005).
9. H. Matsumoto, H. Kageyama, and Y. Miyazaki, *Chem. Commun. (Cambridge)*, **2002**, 1726.
10. M. Matsumoto, M. Yanagida, K. Tanimoto, M. Nomura, Y. Kitagawa, and Y. Miyazaki, *Chem. Lett.*, **2000**, 922
11. R. Del Sesto, C. Corley, A. Robertson, and J. Wilkes, *J. Organomet. Chem.*, **690**, 2536 (2005).
12. C. Bradaric, A. Downard, C. Kennedy, A. Robertson, and Y. Zhou, *Green Chem.*, **5**, 143 (2003).
13. K. Tsunashima and M. Sugiya, *Electrochem. Commun.*, **9**, 2353 (2007).
14. K. Tsunashima and M. Sugiya, *Electrochem. Solid-State Lett.*, **11**, A17 (2008).
15. J. O. Besenhard, *Handbook of Battery Materials*, Wiley-VCH, Weinheim (1999).
16. A. Despic, J. Diggle, and J. Bockris, *J. Electrochem. Soc.*, **115**, 507 (1968).
17. M. Rohnke, T. Best, and J. Janek, *J. Solid State Electrochem.*, **9**, 239 (2005).
18. Y. Zhang and J. Abys, *Modern Electroplating*, 4th ed., John Wiley & Sons, New York (2000).
19. D. Tench and D. Anderson, *Plat. Surf. Finish.*, **77**, 44 (1990).
20. M. Kamitani, T. Koga, and H. Tsuji, *Plat. Surf. Finish.*, **72**, 31 (1985).
21. K. Doyle, C. Lang, K. Kim, and P. Kohl, *J. Electrochem. Soc.*, **153**, A1353 (2006).
22. S. Yoon, J. Lee, S. Kim, and H. Sohn, *Electrochim. Acta*, **53**, 2501 (2008).
23. K. Kim, C. Lang, and P. Kohl, *J. Electrochem. Soc.*, **152**, E56 (2005).
24. C. Scordillis-Kelley, J. Fuller, R. Carlin, and J. Wilkes, *J. Electrochem. Soc.*, **139**, 694 (1992).
25. R. Robinson and R. Stokes, *Electrolyte Solutions*, 2nd ed., Academic Press, New York (1959).
26. T. Riechel and J. Wilkes, *J. Electrochem. Soc.*, **139**, 977 (1996).
27. B. Garcia, S. Lavalle, G. Perron, C. Michot, and M. Armand, *Electrochim. Acta*, **49**, 4583 (2004).